

Photoluminescence of CdS:V,Cu crystals

D. Buhmann, H.-J. Schulz, and M. Thiede

Fritz-Haber-Institut der Max-Planck-Gesellschaft, Teilinstitut für Elektronenmikroskopie, Berlin-Dahlem, Germany

(Received 18 December 1978)

In CdS, vanadium on a cadmium site of C_{3v} symmetry represents a center at which various luminescence processes take place at low temperatures. In the present case, copper acceptors also participate. Two emission bands with zero-phonon structures at $\bar{\nu} = 8681 \text{ cm}^{-1}$ and $\bar{\nu} = 4921 \text{ cm}^{-1}$ are ascribed to internal transitions within the V^{3+} ion, i.e., to transitions between levels which are produced in the crystal field by splitting of the degenerate 3F term of the free ion: ${}^3T_1(F) \rightarrow {}^3A_2(F)$ and ${}^3T_2(F) \rightarrow {}^3A_2(F)$, respectively. A further broad emission band at $\bar{\nu} = 14500 \text{ cm}^{-1}$ seems to involve a vanadium donor which is part of an associated center. The calculated Tanabe-Sugano diagrams allow an interpretation of the measured excitation spectra and yield fitted Racah and crystal-field parameters. Charge-transfer processes for vanadium and copper ions are discussed in the band model.

I. INTRODUCTION

The optical properties of $3d$ transition metals in II-VI compounds have been of practical and theoretical interest for quite some time now.¹ They are fairly well known for systems with plain electron configurations, such as $\text{Cu}^{2+} 3d^9$. However, only a few investigations have been made of the vanadium impurity, and it is presently not clear whether the available results should be ascribed to the charge state $V^{2+} 3d^3$ or to $V^{3+} 3d^2$.

The first publications on vanadium-doped II-VI compounds are by Avinor and Meijer^{2,3}; they describe the emission and the excitation of phosphors (CdS, CdSe, ZnS, ZnSe) at $T=80 \text{ K}$. Absorption spectra of vanadium have been reported at liquid- N_2 temperature for CdTe,⁴ and CdSe,⁵ and at liquid-He temperature for CdS,⁶ ZnSe,^{7,8} ZnS,⁸ CdSe,⁸ and CdTe.⁸ More recently some emission spectra of vanadium in CdSe, CdTe, ZnS, and ZnSe at low temperatures have also been published.⁸ In EPR measurements on vanadium-doped II-VI compounds (CdS, ZnS, ZnSe, ZnTe, ZnO) the trivalent charge state⁹⁻¹⁴ prevails, but the bivalent state^{15,16} is found as well.

In this paper, the luminescence properties of the vanadium in CdS crystals at low temperatures are studied. For the first time, sharp zero-phonon structures in emission are reported. In addition to the known 4800 cm^{-1} band, a new emission band occurs around 8500 cm^{-1} . A crystal-field model for V^{3+} is proposed which allows one to interpret the presented emission and excitation measurements. Moreover, some conclusions are drawn regarding the positions of the ground levels of the V^{3+} and Cu^{2+} ions (which are simultaneously

introduced) with respect to the energy bands of CdS.

II. EXPERIMENTAL DESIGN

The emission measurements were carried out on a 1-m grating spectrometer (Czerny-Turner scanning, Jarrell-Ash Model No. 78-460); the best resolution of this instrument with a grating of 600 lines per mm is about 0.03 nm in first order. The luminescence was excited by an argon laser (Spectra-Physics Model No. 171-18) with various emission lines in the region from 19500 to 22000 cm^{-1} ; the output power was 1 W/line in most experiments. An uncooled PbS photoresistor served as a detector. All emission spectra were corrected with respect to the spectral response of the PbS detector and of the grating efficiency.

Excitation spectra were obtained by means of a double-prism spectrometer (Zeiss Model No. MM 12 with glass prisms). The radiant flux of the exciting radiation was kept constant by means of an automatic slit control; a xenon high-pressure lamp served as the light source. The light emitted from the crystal was again detected by an uncooled PbS photoresistor, and the emission bands were selected by interference filters. For all measurements, the crystals were situated in a helium immersion cryostat.

The crystals were grown from the gaseous phase, and doped by adding vanadium to the initial material. Both copper and nickel were introduced randomly into the crystals in weak concentrations. It is known that copper and vanadium facilitate their incorporation mutually, i.e., act as an activator-coactivator system.^{2,17} The accidental,

very low nickel concentration allowed us to observe narrow Ni^{2+} zero-phonon absorptions at $12\,200\text{ cm}^{-1}$.¹⁸

III. RESULTS OF MEASUREMENTS

The survey spectrum (Fig. 1) shows the emissions in cadmium sulphide in the energy range between 4400 and 8800 cm^{-1} at two different excitation energies. Several regions of emission can be distinguished: At $20\,990\text{ cm}^{-1}$ excitation (lower part of the figure), the typical Cu^{2+} emission prevails, characterized by its peaks near 6200 and 5400 cm^{-1} .¹⁹ At $19\,440\text{ cm}^{-1}$ excitation (upper part of Fig. 1), while the Cu^{2+} structures still remain visible, the bands at 4800 and 8500 cm^{-1} are dominant. They will be attributed to vanadium.

Mainly in the upper part of Fig. 1, a broad background emission is superposed upon the mentioned bands. Its dependence on excitation energy points towards an explanation involving a charge transfer for one of the impurity ions present. Though not a subject of the present study, this background will be investigated in the future and checked against a speculative interpretation which attributes the emission in the $5500\text{--}7000\text{ cm}^{-1}$ range to Ni^+ and the emission in the $7300\text{--}7800\text{ cm}^{-1}$ range to Ni^{2+} centers.

In Fig. 2, the dependence on excitation is demonstrated for the three zero-phonon lines of the vanadium and copper emission bands. The peak

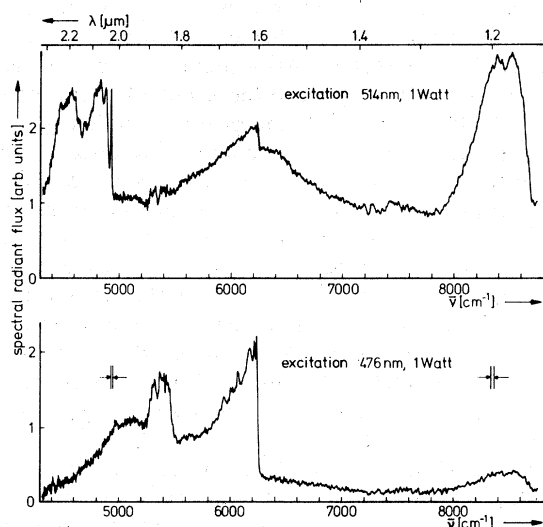


FIG. 1. Emission spectra of CdS:V,Cu at $T \approx 5\text{ K}$; laser excitation. Upper part: vanadium emission bands around 4800 and 8500 cm^{-1} , respectively; excitation at $\lambda = 514\text{ nm}$ ($\bar{\nu} = 19\,440\text{ cm}^{-1}$). Lower part: copper emission bands around 5400 and 6000 cm^{-1} , respectively; excitation at $\lambda = 476\text{ nm}$ ($\bar{\nu} = 20\,990\text{ cm}^{-1}$). The indicated spectral slit width is the same for both spectra.

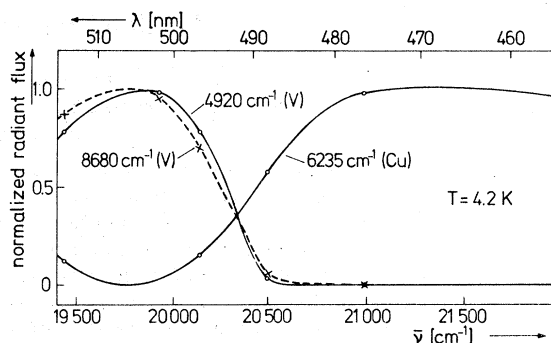


FIG. 2. Excitation spectra of Cu^{2+} and V^{3+} emissions for CdS in the band-edge region. The emission bands were excited by laser radiation and the heights of the zero-phonon peaks were taken as a measure of the radiant flux.

heights of the zero-phonon lines, taken as a measure of the radiant flux, were plotted versus the spectral position of the laser excitation. It can clearly be seen that the Cu emission has a response to the exciting radiation which indicates a competition with the other two emissions plotted. These have virtually identical excitation spectra here; for this reason as well, both emissions are attributed to the same center, formed by a vanadium ion. It should be emphasized that the copper can be excited by band-to-band transitions ($\bar{\nu} \geq \bar{\nu}_{\text{gap}} = 20\,800\text{ cm}^{-1}$) whereas the vanadium emits only on excitation with smaller photon energies ($\bar{\nu}_{\text{max}} = 19\,800\text{ cm}^{-1}$).

Figure 3 shows the entire excitation spectra of the vanadium and copper emissions. The excita-

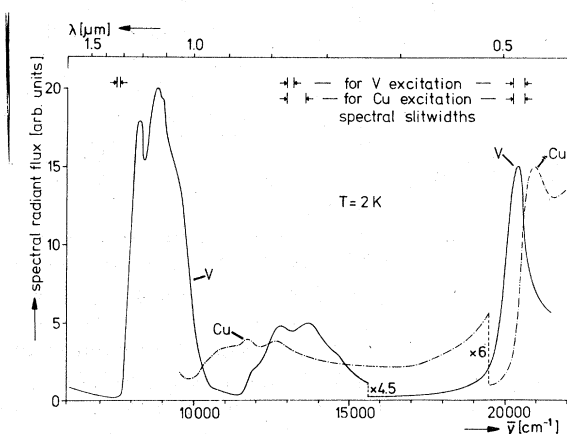


FIG. 3. Excitation spectra of Cu^{2+} and V^{3+} emissions in CdS. The emissions were selected by interference filters in the region from 4300 to 5100 cm^{-1} (V^{3+}) and 5100 to 7500 cm^{-1} (Cu^{2+}), respectively. The spectra are normalized to an equal radiant flux in the band-edge region (around $20\,500\text{ cm}^{-1}$).

tion spectrum of the V emission at $T=2$ K is in very good agreement with the excitation spectrum published for $T=80$ K in Ref. 3 and with the absorption spectrum at $T=4.2$ K in Ref. 6. The broad band^{3,6} in the region from 8000 to 10000 cm^{-1} can mainly be ascribed^{3,20} to the transition ${}^3A_2(F) \rightarrow {}^3T_1(F)$ within the V^{3+} ion, as will be substantiated in the following. In the region between 10000 and 15000 cm^{-1} , transitions at both Cu and V centers superpose; the higher energy transitions among those must, however, preferentially be ascribed to the trivalent vanadium ion (full line).

Due to the low copper concentration, the Cu excitation spectrum is very weak, and it is difficult to determine the positions of the maxima (notice, e.g., the large spectral slit width for these measurements at 13000 cm^{-1}). Nevertheless, a comparison with the Cu excitation spectrum²¹ shows fairly good agreement in the region around 12000 cm^{-1} . In the band-edge region (20000 to 21000 cm^{-1}), the different excitation behavior of Cu and V emissions is pronounced again, as in Fig. 2. The displacement of the maxima compared to Fig. 2 can be explained by the broad-band filtering of the emissions.

In connection with the measurements for Fig. 3, it was unavoidable that, in addition to the V emission at 4800 cm^{-1} , also the low-energy tail of the Cu emission was detected, since the V emission is situated on the shoulder of this Cu emission (cf. Fig. 1, bottom). Therefore, in some of the V excitation spectra an additional maximum at 6600 cm^{-1} shows up, which is merely due to the absorption band of the Cu^{2+} .

In Table I, the obtained excitation maxima of the vanadium luminescence as well as the zero-phonon lines of the emission bands are compiled together with the crystal-field transitions attributed to them. Interpretations in terms of crystal-field transitions were published previously for some of these,^{6,20} but the proposed identifications will be

derived jointly in the discussion.

Parts of the known emission band around 4800 cm^{-1} are shown in Figs. 4 and 5 with increasing resolution. The vanadium emission no longer occurs for excitation with $\bar{\nu} > 20500$ cm^{-1} when the spectral position of the laser line is varied (Fig. 4; cf. Fig. 2). The zero-phonon doublet of this emission is situated at 4918 and 4923 cm^{-1} , respectively, and its lines are differently polarized (Fig. 5). The spacing of the two lines corresponds to the splitting of the ground level at the symmetry reduction $T_d \rightarrow C_{3v}$, as will be discussed later.

One of the crystals used (No. 4013) exhibits an additional "zero-phonon" line at $\bar{\nu}=5038$ cm^{-1} . It may tentatively be ascribed to V centers in a disturbed surrounding since this crystal seems to be less well structured than No. 4011, both in appearance and emission spectrum. The same phonon with about $\hbar\omega_1 = 48 \pm 2$ cm^{-1} , involved in three satellites of the main zero-phonon doublet near 4921 cm^{-1} , seems to be coupled to this additional zero-phonon line at 5038 cm^{-1} as well. This phonon energy is close to the values of 51 cm^{-1} ,²² or 45 cm^{-1} ,²³ respectively, which have been attributed to TA modes of CdS. In a distance of $\hbar\omega_2 = 290 \pm 10$ cm^{-1} from the doublet, the prominent peak near 4630 cm^{-1} (cf. Fig. 1) appears, which again exhibits additional satellites shifted by $\hbar\omega_1$. The energy of $\hbar\omega_2$ compares with the values of 297 cm^{-1} ,²² and of 298 cm^{-1} ,²³ which were obtained for LO phonons previously. The phonon energies $\hbar\omega_1$ and $\hbar\omega_2$ are sufficient to explain all the reproducible fine structure observed in this spectral region.

The new emission around 8500 cm^{-1} displays a fine structure as well (Fig. 6). The zero-phonon transition at 8681 cm^{-1} was recorded with the same resolution as that in Fig. 5 (2 cm^{-1}) and turned out to be a singlet being mainly polarized with an orientation $\vec{E} \perp \vec{c}$. This emission is ascribed to a transition of the trivalent vanadium as well, because it is displayed only by crystals which show

TABLE I. Observed V^{3+} transitions in emission and excitation spectra of CdS:V, Cu at low temperatures. The energy levels are designated taking into account the crystal field of T_d symmetry only; for spin-orbit and C_{3v} interactions see discussion.

	Energetic position (cm^{-1})	Transition (T_d symmetry only)	Polarization
Zero-phonon lines in emission	4918	${}^3T_2(F) \rightarrow {}^3A_2(F)$	$\vec{E} \parallel \vec{c}$
	4923	${}^3T_2(F) \rightarrow {}^3A_2(F)$	$\vec{E} \perp \vec{c}$
	8681	${}^3T_1(F) \rightarrow {}^3A_2(F)$	$\vec{E} \perp \vec{c}$
Excitation maxima of the emission at 4800 cm^{-1}	8250	${}^3A_2(F) \rightarrow {}^1E(D)$	
	8820	${}^3A_2(F) \rightarrow {}^3T_1(F)$	
	9500	${}^3A_2(F) \rightarrow {}^3T_1(F)$	
	12700	${}^3A_2(F) \rightarrow {}^1A_1(G)$	
	13700	${}^3A_2(F) \rightarrow {}^1T_2(D)$	
	14500	${}^3A_2(F) \rightarrow {}^3T_1(P)$	

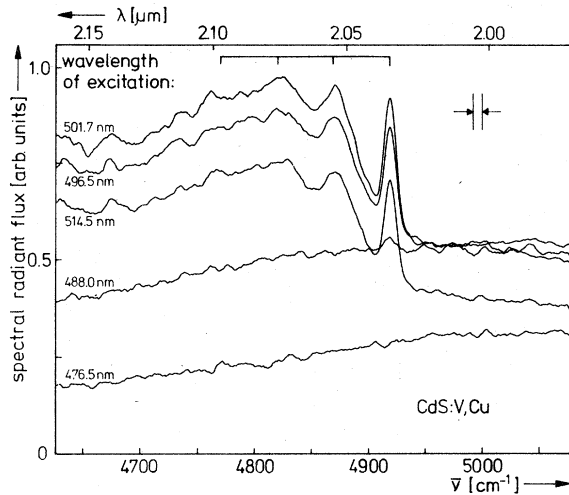


FIG. 4. Vanadium emission around 4800 cm^{-1} at 1-W laser excitation power and $T \approx 5\text{ K}$. Excitation lines: $\lambda = 476.5\text{ nm}$ ($\bar{\nu} = 20990\text{ cm}^{-1}$), 488.0 nm (20490 cm^{-1}), 496.5 nm (20140 cm^{-1}), 501.7 nm (19930 cm^{-1}), 514.5 nm (19440 cm^{-1}).

the $4800\text{-cm}^{-1}\text{ V}^{3+}$ emission, and because these two emissions have a nearly identical excitation behavior (cf. Fig. 2). Apart from the zero-phonon transition, reproducible satellite maxima occur which again may be explained by coupling with the mentioned TA mode $\hbar\omega_1 = 48\text{ cm}^{-1}$. A further pronounced maximum in a distance of $\hbar\omega_3 = 242 \pm 5\text{ cm}^{-1}$ seems to involve the TO phonon, which is

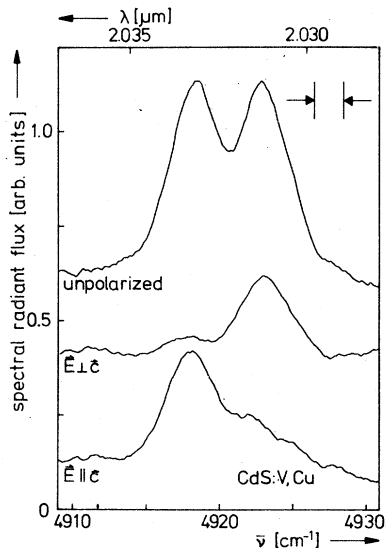


FIG. 5. Zero-phonon doublet of the 4800 cm^{-1} vanadium emission band and polarization of its components. 1-W laser excitation power at $\lambda = 501.7\text{ nm}$ ($\bar{\nu} = 19930\text{ cm}^{-1}$) and $T \approx 5\text{ K}$.

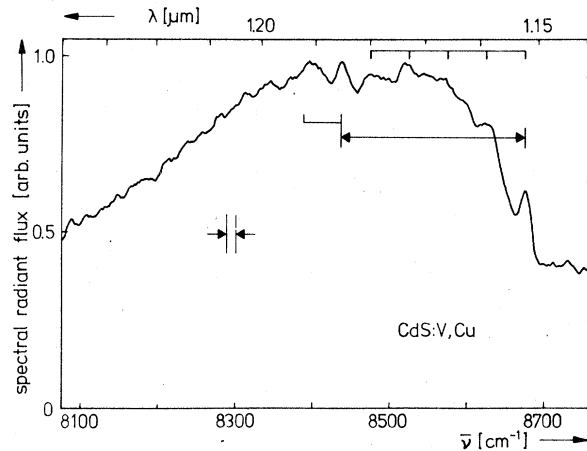


FIG. 6. Vanadium emission around 8500 cm^{-1} with zero-phonon transition at 8681 cm^{-1} . $T \approx 5\text{ K}$, 1-W laser excitation power. Scans with various excitation lines have been averaged.

quoted as 238 cm^{-1} ,²² and as 240 cm^{-1} ,²³ respectively.

In the same spectral region, i.e., near 8500 cm^{-1} , previously²⁴ an emission band in specially pretreated CdS:Cu crystals was found also. The authors tried to interpret this emission as a transition within an associated center comprising copper and another unknown defect. Both the excitation spectrum and the pretreatment of those crystals differ, however, from the conditions for CdS:V,Cu in the present study; a different emission center therefore seems to have been involved in Ref. 24.

Finally, in the spectral region from 13000 to 17000 cm^{-1} , two broad emission bands occur which show an excitation behavior similar to that of the infrared Cu^{2+} and V^{3+} emissions. Selection of proper laser excitation energy leads to a preponderance of one or the other of these bands for the same crystal (Fig. 7). By irradiation with higher-energy photons (at $\bar{\nu} = 20490\text{ cm}^{-1}$), primarily a band at 16000 cm^{-1} is excited, whereas under irradiation in the region of smaller photon energies (19440 cm^{-1}) a band around 14500 cm^{-1} prevails.

Several authors²⁵⁻²⁹ investigated emissions in this spectral region and proposed various models for the respective emission centers. In all the models a lattice defect (V_{Cd} , V_{S} or Cd_i ; V stands for vacancy here) is involved; some authors ascribe the emissions to self-activated centers,²⁷ i.e., complexes formed by a cadmium vacancy (V_{Cd}) and an impurity or to other types of associated centers.²⁸ With this assumption, the experimental evidence presented above suggests that the impurity involved may be a copper ion (16000

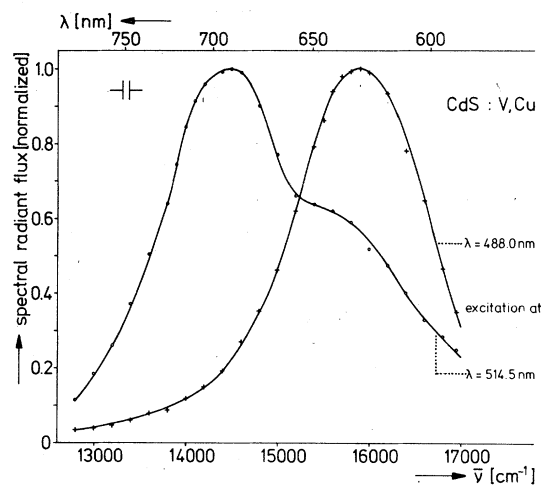


FIG. 7. Emission bands in the visible range at $T \approx 5$ K, 0.7-W laser excitation power at $\lambda = 488$ nm ($\bar{\nu} = 20490$ cm^{-1}) and 514.5 nm (19440 cm^{-1}), respectively.

cm^{-1} band) or a vanadium ion (14500 cm^{-1} band). These emissions in the visible range are, however, not the subject of this paper and will not be discussed in more detail, since they do not represent internal transitions within the V or Cu ions.

IV. DISCUSSION

A. Crystal-field model

For the interpretation of the presented emission and excitation measurements a level scheme is suitable which is based on the electron configuration $3d^2$, i.e., the trivalent charge state of the vanadium. On this premise the assignments are given of the individual measured maxima corresponding to the crystal-field transitions which occur (Table I). Whereas in emission zero-phonon lines have been resolved which are a fairly distinct measure of transition energies, the comparatively broad excitation bands involve phonon interactions. Within the accuracy of the following arguments, however, the excitation maxima suffice to scale the level diagrams.

A Tanabe-Sugano³⁰ diagram has been constructed for V^{3+} (Fig. 8). In the left-hand part, the splittings by combined action of a tetrahedral crystal field and spin-orbit coupling are demonstrated. The diagram was calculated with the energy matrices given in Ref. 31. The vertical line at $Dq/B = 1.45$ represents the best fit of the parameter Dq to the measured transitions. On the right-hand side, the energy levels are derived from the intersections of the eigenvalue curves with the vertical line corresponding to $Dq = 580$ cm^{-1} . For comparison, the measured excitation energies of the 4800

cm^{-1} emission are included and the respective transitions are represented by arrows.

Two separate regions of excitation represent internal transitions, namely, at 8250–9500 cm^{-1} and at 12700–14500 cm^{-1} (cf. Figs. 3 and 8). In the first band, in addition to sublevels of the ${}^3T_1(F)$ term, also the ${}^1E(D)$ level appears, and that below the ${}^3T_1(F)$ levels. It thus supplies an important clue to the arrangement of the observed transitions in a V^{3+} level scheme (see also below). In particular, it is a comparatively narrow excitation band; this fact suggests an explanation in terms of a transition between levels evolving nearly parallel in the Tanabe-Sugano diagram.

The second excitation band is composed of transitions to a component of the 1G term, to the ${}^1T_2(D)$ level, and to the ${}^3T_1(P)$ sublevels. Since these transitions are weak, a superposition of Cu^{2+} transitions (cf. Fig. 3) cannot completely be excluded. A comparison with the vanadium absorption spectrum in Ref. 6 suggests, however, that the measured excitation maxima be interpreted as V transitions. It should be noted that an absorption band corresponding to the 4800- cm^{-1} emission has, up to now, not yet been found. Nor could zero-phonon transitions be observed in absorption at 4921 and 8681 cm^{-1} , respectively.

Nevertheless, both of the corresponding emissions can be interpreted in the Tanabe-Sugano diagram as transitions terminating at the ground level (Fig. 9): the 4921- cm^{-1} emission is assigned to a ${}^3T_2(F) \rightarrow {}^3A_2(F)$ transition, and the 8681- cm^{-1} emission is assigned to a ${}^3T_1(F) \rightarrow {}^3A_2(F)$ transition. The empirical transition energy of 4921 cm^{-1} is considerably smaller than the corresponding calculated quantity of 5750 cm^{-1} (cf. Fig. 8). This is, however, not unusual for electronic systems where Jahn-Teller interactions influence the position of the lower energy levels. This effect is obviously not included in the Tanabe-Sugano splitting scheme.

A discussion of the zero-phonon structures in emission requires a consideration of the symmetry reduction $T_d \rightarrow C_{3v}$: the ground level $T_2({}^3A_2)$ splits into the components Γ_1 and Γ_3 (Bethe's notation), which are separated by $\Delta\bar{\nu} = 5$ cm^{-1} . In EPR measurements done on V^{3+} ions in sapphire,³² a value of 10 cm^{-1} has been found for this splitting, and a theoretical estimate³³ suggests for preferential octahedral symmetry an order of 1 to 10 cm^{-1} for the splitting by a trigonal component of the crystal field. The higher levels also partly split or shift. In Fig. 9 these splittings are schematically shown on the right together with the experimentally found zero-phonon transitions. As a consequence of the selection rules for electric dipole transitions in the point group C_{3v} , emissions leading to the ground level components Γ_1 and Γ_3 are allowed for

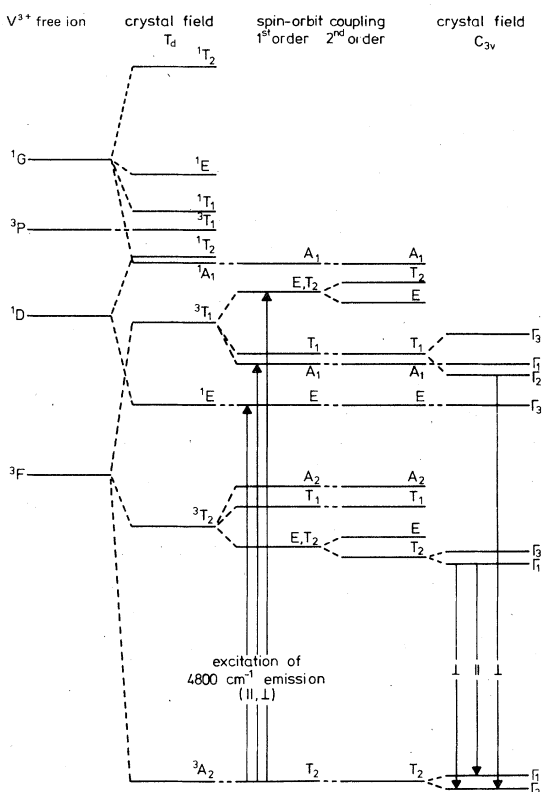


FIG. 9. Energy-level scheme for a d^2 electronic system with splittings by a crystal field of C_{3v} symmetry. On the right-hand side, the observed zero-phonon transitions in emission are shown; in the center, some transitions of the excitation spectrum of the 4800 cm^{-1} emission. The transitions of the 13000 cm^{-1} excitation band have been omitted here for clarity.

sitions ${}^4A_2(F) \rightarrow {}^4T_1(F)$ and ${}^4A_2(F) \rightarrow {}^4T_2(F)$ in the $3d^3$ term scheme.^{8,20} Hence, assuming V^{2+} , both emissions should start from the same energy level ${}^4A_2(F)$ which is thus pushed at least to a position 8681 cm^{-1} above the ground level. Of course, this level cannot be excited by an irradiation at lower energies as would be implied by excitation of the 4800 cm^{-1} emission band by 8250 cm^{-1} irradiation. The occurrence of a second emission band near 8500 cm^{-1} and its incorporation into a common level diagram with the 4800 cm^{-1} band thus seem to exclude the use of the V^{2+} model for the interpretation of the measurements.

To fit the parameters B , C , Dq , and λ to the results of the measurements, series of Tanabe-Sugano diagrams have been calculated for the d^2 configuration by varying the Racah parameter B between 300 and 700 cm^{-1} and C between 1500 and 3000 cm^{-1} . Then, the optimum fit was determined by proper selection of Dq , as in Fig. 8. The value of the spin-orbit coupling constant λ was mainly

obtained from the distance of the excitation structures of the ${}^3T_1(F)$ band at 8820 and 9500 cm^{-1} . The derived parameters are $B = 400\text{ cm}^{-1}$, $C/B = 6.25$, $\lambda = 180\text{ cm}^{-1}$, and $Dq = 580\text{ cm}^{-1}$. The reduction of the Racah parameter B in the crystal field is $B/B_0 = 0.46$ when a value of $B_0 = 861\text{ cm}^{-1}$ is used for the free ion.³⁴

Though Tanabe-Sugano calculations were initially carried out without spin-orbit interaction, its inclusion seems to be justified by effecting the splitting of the ${}^3T_1(F)$ level while conserving the gross character of the diagram. On taking spin-orbit interaction into account, however, a $\lambda = 180\text{ cm}^{-1}$ results which is larger than the free ion value of about 107 cm^{-1} .^{34,35} This is fairly surprising at first sight but agrees on the other hand with the findings for the isoelectronic Ti^{2+} in CdS,^{36,37} and similar host lattices.^{37,38} Hence, at this stage, a dynamic Jahn-Teller interaction in the ${}^3T_1(F)$ level may be offered again as a tentative explanation of these numbers, a quantitative treatment being left to future investigations.

B. Band model (charge-transfer effects)

The measured vanadium excitation bands with $\bar{\nu} \approx 16000\text{ cm}^{-1}$ (cf. Fig. 3) have been interpreted as internal transitions within the V^{3+} ion. In the region from 16000 to about 19000 cm^{-1} , the emission is not excitable. Since according to Fig. 8, energy levels are still present in this region, this suggests that at least above 16000 cm^{-1} the absorption leads to photoionization. Therefore, the positions of the impurity levels within the band gap should be discussed both for the vanadium and the copper ions.

Experimental material on the distances of the Cu levels from the CdS band edges is available from previous papers on the ir emission of Cu^{2+} , e.g., Ref. 39). The rise of the luminescence excitation at $\bar{\nu}_p = \nu_p/c = 9700\text{ cm}^{-1}$ characterizes the threshold energy for the ionization of a hole from the T_2 ground level:



Subsequent trapping of the hole at the ir luminescence center produces the excited state $(Cu^{2+})^*$ in which the hole is situated on the E level:



Hence, luminescent recombination with ir emission finally becomes possible while the Cu^{2+} ion reattains its ground state:



The position of the T_2 ground level of the Cu^{2+} ion 9700 cm^{-1} above the valence band as thus obtained can be confirmed: the sum of this energy distance

and the energy of the "G-Cu" emission⁴⁶ (which also occurs for the crystals studied here) is in fair agreement with the band-gap energy of CdS, i.e., $\bar{\nu}_{\text{gap}} = 20\,800\text{ cm}^{-1}$ at low temperatures. Within the accuracy required, it is unimportant whether this emission could possibly be ascribed to a donor-acceptor pair transition, since the involved donor level would be shallow in any case. To eliminate Franck-Condon shifts, the approximate upper limit of the emitted photons with $\bar{\nu}_e = \nu_e/c \approx 11\,000\text{ cm}^{-1}$ must be used instead of the band maximum at $9\,700\text{ cm}^{-1}$,⁴⁰ although no zero-phonon line has been found at this emission as yet:



Most interestingly, a steep increase in the excitation spectrum²¹ of the ir emission at the same energy indicates that the absorption process inverse to the "G-Cu" emission—i.e., a photoionization of Cu^+ —would enhance the excitation of the Cu^{2+} ir emission by the processes characterized by reactions (1a) and (1b):



For $\text{ZnS}:\text{Cu}^{2+}$ this effect is known as "sensibilization of the Cu^{2+} emission."⁴¹

For the excitability of the Cu^{2+} ir emission in the region of host lattice absorption, as proven by Fig. 3, the processes (1b), (1c), and (2a) can now be considered. These allow a recombination of the generated electron-hole pairs at the Cu centers independent of their initial state of ionization. With the beginning of these processes at $\bar{\nu} > 20\,000\text{ cm}^{-1}$, the excitation yield of the V^{3+} emission decreases considerably (cf. Fig. 2). This suggests low trapping cross sections of the vanadium centers for free carriers.

Finally, it is not possible to say whether the peak at $\bar{\nu} = 19\,800\text{ cm}^{-1}$ in the excitation spectrum of the V^{3+} emission is due to charge transfer transitions or whether internal V^{3+} transitions are involved, say, from the $T_2(3A_2)$ ground level to the T_2 and E components of 1G . Actually, the position of the V^{3+} ground level relative to the bands of CdS is not yet clear. Because of the competing processes at Cu centers [absorptions (1a) and (2b)], even photoconduction spectra are not suitable means for a clarification of this question; deep-level transient spectroscopy, however, could possibly solve this problem.

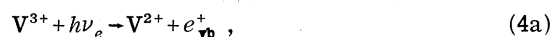
Transmission spectra of the crystals showing the V^{3+} emissions exhibited, in good agreement with the vanadium absorption spectra published previously,⁶ edgeline structures at $\bar{\nu} = 10\,500\text{ cm}^{-1}$ and at $\bar{\nu} = 15\,400\text{ cm}^{-1}$. These might correspond to charge transfer transitions. Assuming one of these values for the photoionization of V^{3+} , the sequence



would be comparable to the processes (1a)–(1c). However, in addition to the uncertainty as to the photoionization energy $h\nu_e$, the intermediate appearance of V^{4+} is hypothetical as well. The excitation spectra which exhibit no maxima at $10\,500$ or $15\,400\text{ cm}^{-1}$, respectively, show that the recombination (3c) would take place without the emission of radiation.

On the other hand, an interpretation of the above-mentioned absorption thresholds as charge transfer processes of the type (3a) would imply that all the structures in the V^{3+} excitation spectrum above the respective edge energy are transitions terminating in V^{3+} levels which are degenerate with the conduction band.⁶ For the isoelectronic ion Ti^{2+} , such degeneracy has already been suggested by several authors,^{38,42} and for $\text{V}^{2+} 3d^3$ as well.^{43,44} The threshold at $\bar{\nu} = 10\,500\text{ cm}^{-1}$ would thus also explain the weakness of the $14\,500\text{ cm}^{-1}$ excitation band of V^{3+} , which, in the absence of V^{2+} , has been predicted⁴⁵ to exceed the $9\,000\text{ cm}^{-1}$ absorption, namely, by interaction with the conduction band.

Conversely, an excitation process initiated by charge transfer could also proceed with participation of the valence band:



Here, the analogy with the processes (1a)–(1c) would be even more pronounced.

In fact, in the picture of an ionic binding of the CdS lattice, the incorporation of V^{2+} on Cd^{2+} sites and consequently the donor character of the vanadium centers can be understood, if the following charged transfer is assumed:



(effective charges in parentheses). Thus, the simultaneous incorporation of vanadium with the copper acceptor becomes plausible as well:



The interrelated electronic properties of vanadium and copper centers are indeed a consequence of the activation procedure, and in future investigations crystals should be prepared and examined, into which various dopants have been deliberately incorporated along with vanadium.

V. SUMMARY

The present paper reports on emission and excitation measurements on CdS:V,Cu at liquid-helium temperatures. In addition to the known 4800-cm⁻¹ V emission, a new emission band appears at 8500 cm⁻¹. For both emissions, zero-phonon structures can be resolved; this is the first measurement of a zero-phonon transition in emission at a vanadium center in a II-VI compound.

The results of the measurements are interpreted by means of a crystal-field model which starts from the trivalent charge state of the vanadium ion, and evidence is presented that a V²⁺ model does not concur with the data. A Jahn-Teller effect could be active at some of the V³⁺ levels but is not considered quantitatively. Subject to this

supposition, the calculated values of the parameters B , C , Dq , and λ are given. The occurring charge transfer processes provide arguments regarding the ground level positions of V³⁺ and Cu²⁺ centers relative to the energy bands of CdS. For a better understanding of the charge states of the vanadium ion, further measurements should be carried out. EPR measurements to obtain additional information regarding the charge states, as well as decay measurements to determine the lifetimes of the individual emissions, are planned.

ACKNOWLEDGMENTS

The authors wish to thank Dr. R. Broser and L. Haussknecht of this institute for growing and supplying the crystals.

- ¹H.-J. Schulz, *Festkörperprobleme* **7**, 75-107 (1967).
²M. Avinor and G. Meijer, *J. Phys. Chem. Solids* **12**, 211-215 (1960).
³G. Meijer and M. Avinor, *Philips Res. Rep.* **15**, 225-237 (1960).
⁴P. A. Slodowy and J. M. Baranowski, *Phys. Status Solidi B* **49**, 499-503 (1972).
⁵J. M. Langer and J. M. Baranowski, *Phys. Status Sol. B* **44**, 155-166 (1971).
⁶R. Pappalardo and R. E. Dietz, *Phys. Rev.* **123**, 1188-1203 (1961).
⁷E. M. Wray and J. W. Allen, *J. Phys. C* **4**, 512-516 (1971).
⁸Le Manh Hoang and J. M. Baranowski, *Phys. Status Solidi B* **84**, 361-365 (1977).
⁹G. W. Ludwig and H. H. Woodbury, *Solid State Phys.* **13**, 223-304 (1962).
¹⁰W. C. Holton, J. Schneider, and T. L. Estle, *Phys. Rev.* **133**, A1638-A1641 (1964).
¹¹A. Hausmann and E. Blaschke, *Z. Phys.* **230**, 255-264 (1970).
¹²G. Filipovich, A. L. Taylor, and R. E. Coffman, *Phys. Rev. B* **1**, 1986-1994 (1970).
¹³R. Böttcher and J. Dziesiaty, *Phys. Status Solidi B* **57**, 617-626 (1973).
¹⁴J. C. M. Henning and J. H. Den Boef, *Solid State Commun.* **14**, 993-996 (1974).
¹⁵T. L. Estle and M. De Wit, *Bull. Am. Phys. Soc.* **6**, 445 (1961).
¹⁶J. Schneider, B. Dischler, and A. Räuber, *Solid State Commun.* **5**, 603-605 (1967).
¹⁷A. Bril and W. van Meurs-Hoekstra, *Philips Res. Rep.* **17**, 280-282 (1962).
¹⁸I. Broser, R. Germer, and H.-J. Schulz (unpublished).
¹⁹I. Broser, H. Maier, and H.-J. Schulz, *Phys. Rev.* **140**, A2135-A2138 (1965).
²⁰J. W. Allen, *Physica* **29**, 764-768 (1963).
²¹F. J. Bryant and A. F. J. Cox, *Br. J. Appl. Phys.* **16**, 463-469 (1965).
²²M. Balkanski, J. M. Besson, and R. Le Toullec, in *Proceedings of the Seventh International Conference on the Physics of Semiconductors, Paris, 1964* (Academic, New York, 1965), pp. 1091-1099.
²³M. A. Nusimovici and J. L. Birman, *Phys. Rev.* **156**, 925-938 (1967).
²⁴S. G. Patil and J. Woods, *J. Lumin.* **4**, 231-243 (1971).
²⁵B. A. Kulp and R. H. Kelley, *J. Appl. Phys.* **31**, 1057-1061 (1960).
²⁶B. A. Kulp, *Phys. Rev.* **125**, 1865-1869 (1962).
²⁷Y. Shiraki, T. Shimada, and K. F. Komatsubara, *J. Appl. Phys.* **45**, 3554-3561 (1974).
²⁸M. Yamaguchi, *Jpn. J. Appl. Phys.* **15**, 1675-1682 (1976).
²⁹I. B. Ermolovich, G. I. Matvievskaia, and M. K. Sheinkman, *Sov. Phys. Semicond.* **9**, 1070-1071 (1976).
³⁰Y. Tanabe and S. Sugano, *J. Phys. Soc. Jpn.* **9**, 753 (1954); **9**, 766 (1954).
³¹A. D. Liehr and C. J. Ballhausen, *Ann. Phys. (N.Y.)* **6**, 134-155 (1959).
³²G. M. Zverev and A. M. Prokhorov, *Sov. Phys. JETP* **7**, 707-708 (1958).
³³J. H. van Vleck, *J. Chem. Phys.* **7**, 61-71 (1939).
³⁴J. S. Griffith, *The Theory of Transition Metal Ions* (Cambridge University, Cambridge, England, 1961).
³⁵T. M. Dunn, *Trans. Faraday Soc.* **57**, 1441-1444 (1961).
³⁶R. Boyn and G. Ruzsyczynski, *Phys. Status Solidi B* **48**, 643-655 (1971).
³⁷A. Rosenfeld, R. Boyn, and G. Ruzsyczynski, *Phys. Status Solidi B* **70**, 601-610 (1975).
³⁸J. Gardavský, I. Barvik, and M. Zvára, *Phys. Status Solidi B* **84**, 691-698 (1977).
³⁹I. Broser, R. Broser-Warminsky, and H. J. Schulz, in *Proceedings of the International Conference on Semiconductor Physics, Prague, 1960* (Academic New York, 1961), pp. 771-775.
⁴⁰E. Grillot and P. Guintini, *C. R. Acad. Sci.* **236**, 802-804 (1953).
⁴¹I. Broser and H.-J. Schulz, *J. Electrochem. Soc.* **108**, 545-548 (1961).
⁴²R. Boyn, J. Dziesiaty, and D. Wruck, *Phys. Status Solidi B* **42**, K197-200 (1970).
⁴³J. M. Baranowski, J. M. Langer, *Phys. Status Solidi B* **48**, 863-873 (1971).
⁴⁴J. M. Baranowski, J. M. Langer, and S. Stefanova, in *Proceedings of the 11th International Conference on the Physics of Semiconductors, Warsaw, 1972* (PWN Polish Sci., Warszawa, 1972), pp. 1001-1008.
⁴⁵W. E. Hagston, *J. Phys. C* **1**, 818-820 (1968).
⁴⁶This emission is usually labeled "G-Cu" emission since with ZnS the corresponding emission band is in the green spectral region.